Establishment of constitutive model for impact damage of plant fiber reinforced composite materials

João Carlos da Cruz Dias
joao.cruz.dias@tecnico.ulisboa.pt

Instituto Superior Técnico, Universidade de Lisboa, Portugal

November 2021

Abstract

The increasing use of composite materials in the aerospace industry and the growing necessity to obtain greater efficiency and lowering its carbon footprint, green composites (or natural fiber reinforced composites) present a good alternative for use in some internal panels of airplanes allowing for a lower weight and possibly cost of the plane in general. Possible applications are in areas susceptible to impact (lavatories and over-head cargo space linings) and, as such, the study of low velocity impact on plant fiber reinforced composites is important. The development of a constitutive model for low velocity impact that considers the nonlinear behaviour of natural fibers, caused by them being normally used after twisted together into a yarn, allows for a better numerical study of these materials. The model developed is able to consider the yarn nonlinear behaviour introducing it into the Hashin failure criteria via some literature based assumptions. It was possible to use the failure criteria for an off-axis loading case presented by Hashin modifying it to take the twist angle of the reinforcing yarns into consideration. With this, it was possible to numerically analyse the problem with the development of a VUMAT subroutine and the Abaqus/Explicit solver. An analysis for the low velocity impact was made for a sixteen layer unidirectional composite laminate under five different impact velocity cases (correspondent to $5J$, $7J$, $8J$, $9J$ and $10J$) and the results are presented and analysed. Conclusions about the work done, achievements and future work are also presented.

Keywords: Laminated Composite Materials, Natural Fiber, Twist Angle, Low Velocity Impact, Nonlinear behaviour.

1. Introduction

Composite materials are a type of materials widely used for various engineering applications. Some examples of the industries that use this type of materials are the automotive, the naval and the aerospace. Composite materials are a mixture of two or more materials that combine the properties in order to produce a final material with a desired set of properties. This work will focus on the fiber reinforced laminated composite materials, that consist on the stacking of layers of a matrix reinforced with fibers. These fibers have a high strength and high modulus that allow for obtaining a reinforced material.

The combination of materials, allow for the conception of a material that will have the properties that are the most fit for a specific application. The aerospace industry uses these materials as it is possible to obtain a material that has a high strength, high impact energy, good fatigue performance, good corrosion resistance and high fracture toughness, while maintaining a low weight. [1]

As one of the main challenges on aviation nowadays is to reduce the environmental impact, it is beneficial to make the composite materials more ecological using natural fibers as a reinforcement. They have a degradable nature, their sourcing accounts for lower carbon emissions and their production is more energy efficient [2, 3]. They also have mechanical properties, in some cases, similar to glass fibers [4] and they are light-weight due to their low density [5]. This light-weight property makes them an ideal substitute for the use in internal panels (from flooring to lavatories or cargo hold linings) since they can reduce the weight of these components and greatly improve the efficiency of the aircraft, since the lowering of the weight of the aircraft, improves the range, fuel consumption and carbon emissions [6]. All of this allows for the possibility of changing from using synthetic to natural fibers as the reinforcement for composite materials in certain applications, like over head cargo hold or lavatory linings that are subjected to impacts of low velocities which implies a study of it's properties and behaviour.

2. Background

In order to develop a constitutive model for the material behaviour under low velocity impact it's important to consider the material elastic behaviour, it's nonlinear behaviour and also the failure criteria to evaluate the material failure.

2.1. Orthotropy

Composite materials can accumulate damage as it occurs and, as such, it would not be correct to use only the failure criteria to predict the failure behaviour of the material and a Continuum damage model should be applied for the analysis. So, the

$$\sigma_i = C_{ij}\epsilon_j \tag{1}$$

where the engineering parameters, σ_i = stresses, C_{ij} = Stiffness matrix and ϵ_j = strain. Making the orthotropic assumptions from the previous chapters, the tri-dimensional stiffness can be reduced to 9 variables obtaining the stiffness and compliance matrices in the form:

$$[C_{ij}] = \begin{bmatrix} C_{11} & C_{12} & C_{13} & 0 & 0 & 0 \\ & C_{22} & C_{23} & 0 & 0 & 0 \\ & & C_{33} & 0 & 0 & 0 \\ & & & C_{44} & 0 & 0 \\ & & & & C_{55} & 0 \\ Sym. & & & & & C_{66} \end{bmatrix} \tag{2}$$

where, for three directions of a material ($i, j = 1, 2, 3$), the components of the stiffness matrix are [**?**]:

$$C_{11} = \frac{1 - \nu_{23}\nu_{32}}{E_2 E_3 \Delta}\,, \tag{3a}$$

$$C_{12} = \frac{\nu_{21} + \nu_{31}\nu_{23}}{E_2 E_3 \Delta} = \frac{\nu_{12} + \nu_{32}\nu_{13}}{E_1 E_3 \Delta}\,, \tag{3b}$$

$$C_{13} = \frac{\nu_{21} + \nu_{31}\nu_{23}}{E_2 E_3 \Delta} = \frac{\nu_{12} + \nu_{32}\nu_{13}}{E_1 E_3 \Delta}\,. \tag{3c}$$

$$C_{22} = \frac{1 - \nu_{13}\nu_{31}}{E_1 E_3 \Delta}\,. \tag{3d}$$

$$C_{23} = \frac{\nu_{32} + \nu_{12}\nu_{31}}{E_1 E_3 \Delta} = \frac{\nu_{23} + \nu_{21}\nu_{13}}{E_1 E_3 \Delta}\,. \tag{3e}$$

$$C_{33} = \frac{1 - \nu_{12}\nu_{21}}{E_1 E_2 \Delta}\,. \tag{3f}$$

$$C_{44} = G_{12}; \qquad C_{55} = G_{23}; \qquad C_{66} = G_{13}\,. \tag{3g}$$

$$\Delta = \frac{1 - \nu_{12}\nu_{21} - \nu_{23}\nu_{32} - \nu_{31}\nu_{13} - 2\nu_{21}\nu_{32}\nu_{13}}{E_1 E_2 E_3}\,. \tag{3h}$$

2.2. Nonlinear

Shah *et al.* [7] studied the introduction of the twist angle (causing the nonlinear behaviour) both in the Tsai-Hill criteria (Equation 4) and through a squared cosine in the rule of mixtures and fitted to the experimental data (Equation 5).

$$\sigma_\theta = \left[\frac{1}{\sigma_0^2}cos^4(\theta) + \left(\frac{1}{\tau^2} - \frac{1}{\sigma_0^2}\right)cos^2(\theta)sin^2(\theta) + \frac{1}{\sigma_{90}^2}sin^4(\theta)\right]^{-0.5} \tag{4}$$

$$\sigma_\alpha = \cos^2(2\cdot\alpha)\cdot\eta_l V_f \sigma_f + (1 - V_f)\sigma_m \tag{5}$$

The results from these two models for the tensile case considering long fibers are shown in Figure 1

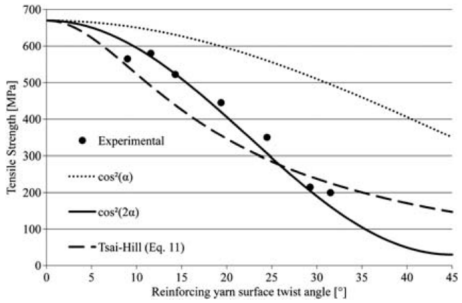

Figure 1: Effect of yarn twist on long flax fibre impregnated yarn. [7]

With this, its possible to assume that even though the modelling of the tensile behaviour of flax fibers using a $cos^2(\alpha)$ fitted to each specific experimental case, the utilization of the off-axis loading of the Tsai-Hill model, with the relatively good fit to the experimental data, allows for the possible introduction of the twist angle in a failure criteria for a general application.

2.3. Hashin Failure Criteria

– **Fibre Mode**

- *Tensile Fibre Mode* $\sigma_{11} > 0$

$$\left(\frac{\sigma_{11}}{\sigma_A^+}\right)^2 + \frac{1}{\tau_A^2}(\sigma_{12}^2 + \sigma_{13}^2) = 1 \tag{6}$$

or,

$$\sigma_{11} = \sigma_A^+ \tag{7}$$

- *Compressive Fibre Mode* $\sigma_{11} < 0$

Considers it to be the simple maximum stress form.

$$\sigma_{11} = -\sigma_A^- \tag{8}$$

– **Matrix Mode**

- *Tensile Matrix Mode* $\sigma_{22} + \sigma_{33} > 0$

$$\frac{1}{\sigma_T^{+2}}(\sigma_{22}+\sigma 33)^2+\frac{1}{\tau_T^2}(\sigma_{23}^2-\sigma_{22}\sigma_{33})+\frac{1}{\tau_A^2}(\sigma_{12}^2+\sigma_{13}^2) = 1 \tag{9}$$

- *Compressive Mode* $\sigma_{22} + \sigma_{33} < 0$

$$\frac{1}{\sigma_T^-}\left[\left(\frac{\sigma_T^-}{2\tau_T}\right)^2 - 1\right](\sigma_{22}+\sigma_{33}) + \frac{1}{4\tau_T^2}(\sigma_{22}+\sigma_{33})^2 + \frac{1}{\tau_T^2}(\sigma_{23}^2 - \sigma_{22}\sigma_{33}) + \frac{1}{\tau_A^2}(\sigma_{12}^2+\sigma_{13}^2) = 1 \tag{10}$$

3. Implementation

3.1. Theoretical Model for the material behaviour

In order to obtain a model that considers the progressive damage of the material during the impact, it is important to calculate the variations in stresses using the variations in strains as well as the damage introduction on the stiffness matrix.

Strains

The strain state alteration is as follows:

$$\epsilon_{new} = \epsilon_{old} + \epsilon_{increment} \tag{11}$$

Where, ϵ_{new} is the strain for the current iteration, ϵ_{old} is the strain for the previous iteration and the $\epsilon_{increment}$ is the strain increment given for the calculations of the current iteration.

Damaged Stiffness Matrix

With the alteration in strains and the damage coefficients calculated from the previous iteration of this process (where in the initial state, the damage coefficients all are equal to 0) the damaged stiffness matrix can be calculated, from Linde *et al.* [8], and are presented in Equation 18

where, d_f is the fiber damage, d_m is the matrix damage and are defined by:

$$d_f = 1 - (1 - d_{ft})(1 - d_{fc}), \tag{12a}$$

$$d_m = 1 - (1 - S_{mc}d_{mt})(1 - S_{mc}d_{mc}), \tag{12b}$$

Where d_f is the fiber damage component in function of the tensile and compressive fiber damage (d_{ft} and d_{fc} respectively). The matrix damage (d_m) is given in function of the tensile and compressive matrix damage (d_{ft} and d_{fc} respectively) and the coefficients S_{mt} and S_{mc} are to control the shear stiffness due to matrix damage and are set as $S_{mt} = S_{mc} = 0.93$ from[9].

Stresses

With the calculation of the strains and the damaged stiffness matrix, it is possible to calculate the new stress state for each iteration:

$$\sigma_i = C_{ij}^d \epsilon_j \tag{13}$$

Failure Evaluation - Hashin Failure Criteria with twist angle effect

For the failure of the composite, the Hashin failure criteria [10] was considered due to it's capacity to evaluate the progress of the damage during testing. Since the nonlinear behaviour of the plant fiber composites has its origin in the twisting of the yarns, it is important to take this twisting into account.

For the introduction of the twist, the Figure 2 shows the simplification process to visualise the simplification of a twisted yarn to a composite plate with off-axis fiber orientation.

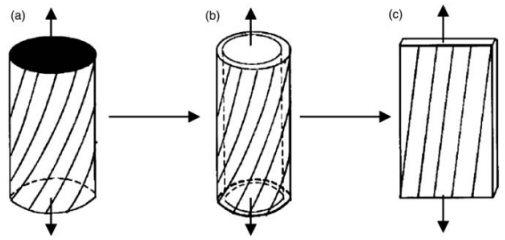

Figure 2: An impregnated yarn is similar to an off-axis composite. (a) twisted impregnated yarn with surface twist angle α, (b) a layer of a twisted impregnated yarn (c) the open-up structure of the layer is a laminate with off-axis loading angle θ. [7]

Considering the Hashi's criteria for off-axis loading:

Fibre Mode

- *Tensile Fibre Mode* $\sigma_{11} > 0$

$$\left(\frac{\sigma_{11}}{\sigma_{fu}}\right)^2 + \frac{1}{\tau_A^2}(\sigma_{12}^2+\sigma_{13}^2) = 1 \tag{14}$$

or,

$$\sigma_{11} = \sigma_{fu} \tag{15}$$

- *Compressive Fibre Mode* $\sigma_{11} < 0$

$$\sigma_{11} = -\sigma_A^- \tag{16}$$

Matrix Mode

- *Tensile Matrix Mode* $\sigma_{22} + \sigma_{33} > 0$

$$\frac{1}{\sigma_{mu}}(\sigma_{22}+\sigma 33)^2 + \frac{1}{\tau_T^2}(\sigma_{23}^2 - \sigma_{22}\sigma_{33}) + \frac{1}{\tau_A^2}(\sigma_{12}^2+\sigma_{13}^2) = 1 \tag{17}$$

$$[C_{ij}^d] = \begin{bmatrix} (1-d_f)C_{11} & (1-d_f)(1-d_m)C_{12} & (1-d_f)C_{13} & 0 & 0 & 0 \\ & (1-d_m)C_{22} & (1-d_m)C_{23} & 0 & 0 & 0 \\ & & C_{33} & 0 & 0 & 0 \\ & & & (1-d_f)(1-d_m)G_{12} & 0 & 0 \\ & & & & (1-d_m)G_{23} & 0 \\ & Sym. & & & & (1-d_f)G_{13} \end{bmatrix} \quad (18)$$

- *Compressive Mode* $\sigma_{22} + \sigma_{33} < 0$

$$\frac{1}{\sigma_T^-}\left[\left(\frac{\sigma_T^-}{2\tau_T}\right)^2 - 1\right](\sigma_{22}+\sigma_{33}) + \frac{1}{4\tau_T^2}(\sigma_{22}+\sigma_{33})^2 + \frac{1}{\tau_T^2}(\sigma_{23}^2 - \sigma_{22}\sigma_{33}) + \frac{1}{\tau_A^2}(\sigma_{12}^2+\sigma_{13}^2) = 1 \quad (19)$$

where,

$$\sigma_{fu} = \frac{1}{cos^2(\theta)\left[\frac{cos^2(\theta)}{\sigma_T^2} + \frac{sin^2(\theta)}{\tau_A^2}\right]} \quad (20)$$

for the fiber ultimate stress,

$$\sigma_{mu} = \frac{1}{sin^2(\theta)\left[\frac{sin^2(\theta)}{\sigma_T^2} + \frac{cos^2(\theta)}{\tau_A^2}\right]} \quad (21)$$

for the matrix ultimate stress.

The angle θ is the angle of the fibers with load direction and this can be obtained with:

$$\theta_{mean} = \alpha + \frac{\alpha}{tan^2(\alpha)} - \frac{1}{tan(\alpha)} \quad (22)$$

As for the value of α (the surface twist angle) it can be obtained by using the staple yarn definition of Hearle *et al.* [11] (where the yarn cross-section is assumed to be circular) by the following equation:

$$tan(\alpha) = \frac{2\pi r}{L} = 2\pi r T \quad (23)$$

where, L is the lenght of the yarn for one turn, r is the fiber radius and T is the twist level (also defined as $1/L$).

Pan [12] on his work states that the surface twist angle of the yarn is better given by 2α due to the double helix configuration that the twisted yarn presents.

3.2. Numerical implementation

In order to simulate the low velocity impact in a flax yarn reinforced laminated composite plate, the numeric solver Abaqus/Explicit was used for the modelling and processing of the test simulation. A user subroutine VUMAT was developed in order to allow for the introduction of the material specific characteristics as well as the modification of the criteria defining the material behaviour in order to implement the modified Hashin failure criteria.

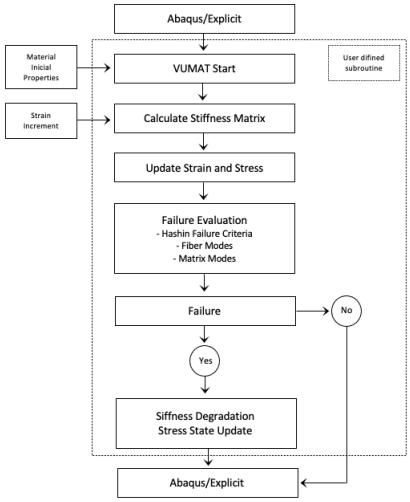

Figure 3: VUMAT user subroutine flow chart for the procedure for the project analysis.

The subroutine, with the basic description shown in Figure 3.2, has the material properties introduced via a $1 \times n$ matrix and are set in the model created in the Abaqus/Explicit CAE environment. This input matrix includes, for the present implementation, the three dimensional material properties for the Elasticity (E) and Shear (G) Moduli, Poisson ratios (ν_{ij}), Ultimate Normal (σ) and Shear (τ) Stresses and Density (ρ).

With the material properties (Table and simulation parameters inserted, the subroutine starts by assuming a purely elastic material and calculates an non-deformed stiffness matrix (C_{ij}) using the Equations 3. With the stiffness matrix and the initial values of the stresses and strains, as well as the ultimate stresses and strains, it proceeds to do a failure evaluation using the Hashin failure criteria (either modified or non-modified, depending on the analysis) and evaluates the damage and if failure is achieved.

With every iteration, a strain increment is imputed from the Abaqus/Explicit model and added to the initial strain. From this, a deformed stiffness matrix is calculated using the model in Equation 18 and the stresses are updated initiating a new failure evaluation.

As an output, the VUMAT allows for the update of the "svd" parameters that, in the present study where set as the outputs for the failure of the various

Property	Value	Units
E_{11}	31.42	GPa
E_{22}	5.58	GPa
E_{33}	5.58	GPa
ν_{12}	0.353	–
ν_{13}	0.353	–
ν_{23}	0.403	–
G_{12}	2.07	GPa
G_{13}	2.07	GPa
G_{23}	1.035	GPa
σ_1^{tu}	286.70	MPa
σ_1^{cu}	127.11	MPa
σ_2^{tu}	33.86	MPa
σ_2^{cu}	79.94	MPa
σ_3^{tu}	33.86	MPa
σ_3^{cu}	79.94	MPa
τ_{12}^{u}	37.35	MPa
τ_{13}^{u}	37.35	MPa
τ_{23}^{u}	37.35	MPa
ρ	1310	kg/m^3
β_{damp}	$1.9E^{-8}$ [13]	–
$cos^2(\theta)$	0.0689	–
$sin^2(\theta)$	0.93106	–

Table 1: Properties used on the definition of the user material.

modes of the Hashin failure criteria. It allows also for the update in the Abaqus/Explicit model of the new stresses, strains and internal energies.

3.3. Validation

For the validation of the proposed model, the experimental procedures and results from Sy *et al.* [14] were considered.

4. Results

The results obtained using the presented model implemented using a VUMAT subroutine and the Abaqus/Explicit solver are demonstrated in this section.

4.1. Energy comparison

Kinetic Energy

In order to validate the absorbed energy after low velocity impact, the final kinetic energy was compared to the initial impact energy and the verified difference is compared to available literature.

$$E_{absorbed} = E_{Inicial} - E_{kinetic_{final}} \tag{24}$$

Comparing the results from Table 2 between the numerical results of Sy *et al.* [15] and the results from the numerical study made using the presented model, it is possible to verify some differences. The energy dissipation caused by the impact is better modelled by the implementation described with the dissipated energy being still an over estimation of the experimental results but being smaller in value creating a smaller error. This might be a consequence of the assumptions made by Sy *et al.* in their work that the material would have a linear behaviour and in the present work, the nonlinear behaviour caused by the twisting of the natural fibers was considered.

Even though the numerical results appear to present small differences when compared to the experimental results, the errors cannot be disregarded and there are some possible explanations for the difference in results. One of which is the manner that the composite was modelled without considering inter-ply interactions. This would have attributed to them an interaction property that would, possibly, predict a different behaviour of the relations between plies when under the impact load introducing failures modes like delamination. Other relates to the approximations and assumptions made regarding the material properties for the application of a three dimensional criteria.

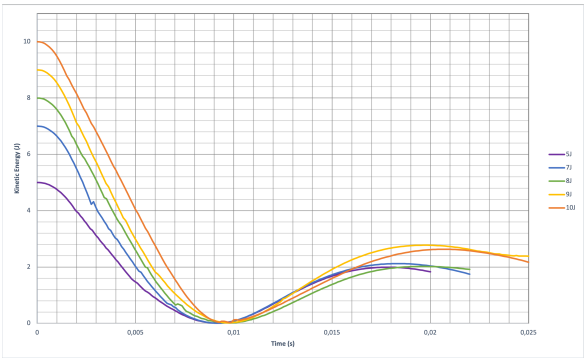

Figure 4: Energy graphs for the impact simulations with the different inicial impact energies.

4.2. Plate deformations

Abaqus/Explicit also allowed for the visualization of the stress evolution, damage and distortion through the plate during the impact analysis.

Figures 5, 6 and 7 show three frames of the analysis in order to represent the composite plate deformation and stress evolution in three points of the simulation.

It is possible to observe the elements distortion and damage on the mentioned images and the disappearing of some elements (that had met the conditions for failure via the Hashin failure criteria, implemented). It is also possible to observe the appearance of a crack on the perpendicular direction to that of the fibers direction. In Figure 9 the example for the fiber compressive failure is illustrated showing elements that met the failure criteria. The deletion of some of these elements might explain the lack of stress concentrations on the edge of the back of the plate in the example from Figure 6, where the

Initial Energy (J)	Absorbed Energy (J)			Difference from experimental (%)	
	Experimental Sy *et al.*	Numerical Sy *et al.*	Studied Model	Sy *et al.*	Studied Model
5	2, 89	3, 12	3, 007	7, 96	4, 04
7	4, 64	4, 74	4, 711	2, 16	1, 53
8	5, 14	5, 67	5, 243	10, 31	2, 00
9	6, 07	6, 51	6, 225	7, 25	2, 55
10	10	7, 41	7, 367	25, 90	26, 33

Table 2: Comparison between absorbed energy obtained using the model proposed in this study and the experimental results obtained by Sy *et al.* [14], and the numerical results obtained by Sy *et al.* [15]

plate support should be cause of some stress concentrations.

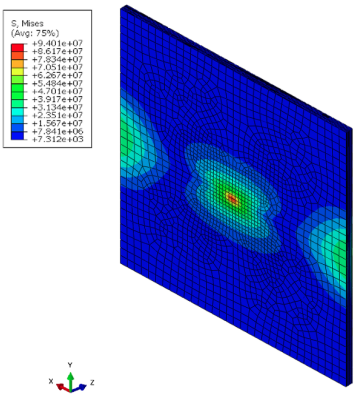

Figure 5: Stress distribution at the beginning of the analysis for initial impact energy of $8J$ (back view).

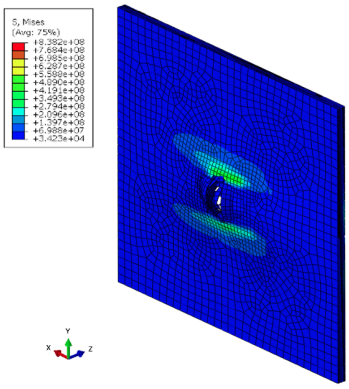

Figure 6: Stress distribution at the middle of the analysis for initial impact energy of $8J$ (back view).

It is possible to observe the elements distortion and damage on the mentioned images and the disappearing of some elements (that had met the conditions for failure via the Hashin failure criteria, implemented). It is also possible to observe the appearance of a crack on the perpendicular direction to that of the fibers direction. In Figure 9 the example for the fiber compressive failure is illustrated showing elements that met the failure criteria. The deletion of some of these elements might explain the lack of stress concentrations on the edge of the back

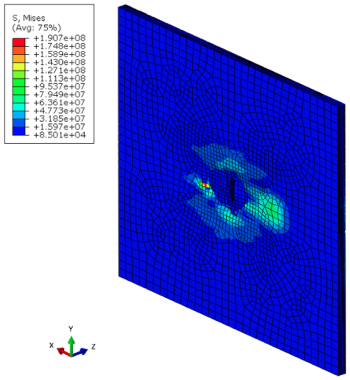

Figure 7: Stress distribution at the end of the analysis for initial impact energy of $8J$ (back view).

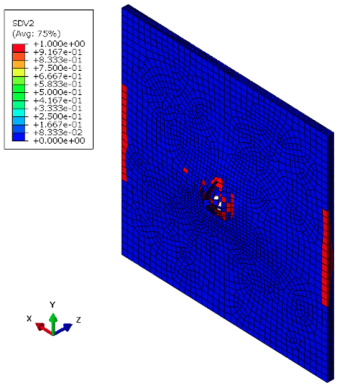

Figure 8: Fiber compressive damage at the middle of the analysis for initial impact energy of $8J$(back view).

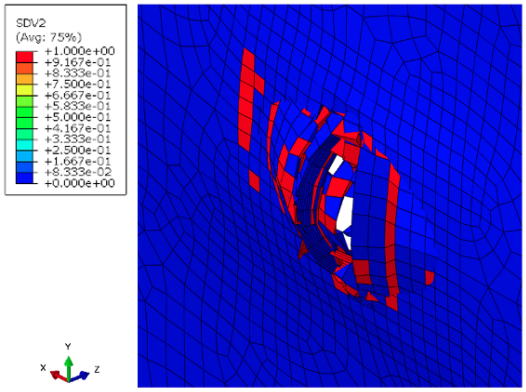

Figure 9: Detailed view of fiber compressive damage at the middle of the analysis for initial impact energy of $8J$(back view).

of the plate in the example from Figure 6, where the plate support should be cause of some stress concentrations.

5. Conclusions

The study and development of the model went through the considerations of various authors for the effects of the twist angle of the yarns reinforcing the fibers and possible implementations. The model then was chosen to be implemented using the Hashin failure criteria. With the introduction of the yarn twist angle into the off-axis form of the Hashin failure criteria, was possible to obtain and implement a model for the damage progression on these types of composites. The validation was made considering results available in literature for low velocity impact on unidirectional composites reinforced by flax fibers.

The implementation of the model, made using Abaqus/Explicit Finite Element Analysis software, was made using the user-defined subroutine VUMAT. It is important to note that for an application like this, it is important to create a model using Abaqus/Explicit that will be used to input into the VUMAT subroutine linking them into a relation where the VUMAT has the model for the material behaviour and Abaqus/Explicit introduces into the VUMAT the material properties and parameters, gives the increments needed to the successive VUMAT iterations and also does the result post processing. Also important, is the necessity of assume the material properties for the three dimensional case.

The author considers that the model and implementation presented in this study is a possible alternative for the study of a plant fiber (yarn) reinforced composite but recognizes that the analysis and validation of the model was limited to the data available on literature for low velocity impact on flax fiber reinforced composites and it is important to experimentally and numerically analyse and simulate cases with the same flax fiber reinforced composites but constituted by yarns with fibers spun in different angle orientations in order to further validate the usefulness of the presented model and expand the scope of analysis to other natural sourced fiber spun into yarns, such as sisal or hemp in order to further validate the presented model. Nonetheless, the results obtained in the analysis performed were consistent to the literature available and showed a good estimation of the material behaviour when subjected to low velocity impact cases in most cases, except the case which the impact energy should cause catastrophic failure of the material which can be attributed to the non consideration of the inter-ply interactions.

5.1. Achievements

The present work's major achievement was the successful development and implementation of a viable model for the study of unidirectional plant fiber (more specifically flax fiber) reinforced composites when subjected to low velocity impacts. The successful validation of the presented and implemented model adds the possibility of using Abaqus/Explicit as a tool for the analysis of these materials which might incentive others to work on the subject, improve the models presented and develop better and more accurate investigation tools.

5.2. Future work

For the future of the investigations on this subject, it would be advantageous to re-think and/or improve some aspects and simplifications of the presented model.

An interesting improvement to the model would be the introduction of the matrix failure modes from Puck into the matrix failure mode of the Hashin failure criteria, in order to better simulate the matrix failure and, possibly, improve the composite total failure.

The creation of a model of the composite plate that would include the inter-ply interactions introducing, for example, cohesive elements between plies. Since this type of study would increase the computational time, would also be interesting to investigate the possibility of extending the VUMAT subroutine to calculate the parameters needed to the utilization of shell elements on the simulation.

Other possible improvement would be the making a mesh refinement study for each of the energy impact cases in order to find the optimal mesh refinement that would provide a good balance between computational time and results accuracy.

References

[1] Sohel Rana and Raul Fangueiro, editors. *Advanced Composite Materials for Aerospace Engineering*. Woodhead Publishing, 2016.

[2] Y. Li and B. Yuan. Nonlinear mechanical behavior of plant fiber reinforced composites. *Journal of Biobased Materials and Bioenergy*, 8, 04 2014.

[3] Hao Ma, Yan Li, and Di Wang. Investigations of fiber twist on the mechanical properties of sisal fiber yarns and their composites. *Journal of Reinforced Plastics and Composites*, 33(7):687–696, 2014.

[4] Hao Ma, Yan Li, Yiou Shen, Li Xie, and Di Wang. Effect of linear density and yarn structure on the mechanical properties of ramie fiber yarn reinforced composites. *Composites Part A: Applied Science and Manufacturing*, 87:98 – 108, 2016.

[5] J.M.F.A. Blanchard and A.J. Sobey. Comparative design of e-glass and flax structures based on reliability. *Composite Structures*, 225:111037, 2019.

[6] P. Balakrishnan, M.J. John, L. Pothen, M.S. Sreekala, and S. Thomas. 12 - natural fibre and polymer matrix composites and their applications in aerospace engineering. In Sohel Rana and Raul Fangueiro, editors, *Advanced Composite Materials for Aerospace Engineering*, pages 365–383. Woodhead Publishing, 2016.

[7] Darshil Shah, Peter Schubel, and Mike Clifford. Modelling the effect of yarn twist on the tensile strength of unidirectional plant fibre yarn composites. *Journal of Composite Materials*, 47:425–436, 02 2013.

[8] Peter Linde, Jrgen Pleitner, Henk Boer, and Clarice Carmone. Modelling and simulation of fibre metal laminates. *ABAQUS Users' Conference*, 01 2004.

[9] Junjie Zhou, Pihua Wen, and Shengnan Wang. Finite element analysis of a modified progressive damage model for composite laminates under low-velocity impact. *Composite Structures*, 225:111113, 2019.

[10] J. P. Boehler and M. Delafin. Failure criteria for unidirectional fiber-reinforced composites under confining pressure. In Jean-Paul Boehler, editor, *Mechanical Behavior of Anisotropic Solids / Comportment Méchanique des Solides Anisotropes*, pages 449–470, Dordrecht, 1982. Springer Netherlands.

[11] J.W.S. Hearle, P. Grosberg, and S. Backer. *Structural Mechanics of Fibers, Yarns, and Fabrics*. Number vol. 1 in Structural Mechanics of Fibers, Yarns, and Fabrics. Wiley-Interscience, 1969.

[12] Ning Pan. Development of a constitutive theory for short fiber yams: Part iii: Effects of fiber orientation and bending deformation. *Textile Research Journal*, 63(10):565–572, 1993.

[13] Md Zillur Rahman. Mechanical and damping performances of flax fibre composites a review. *Composites Part C: Open Access*, 4:100081, 2021.

[14] Benedict Lawrence Sy, Zouheir Fawaz, and Habiba Bougherara. Damage evolution in unidirectional and cross-ply flax/epoxy laminates subjected to low velocity impact loading. *Composites Part A: Applied Science and Manufacturing*, 112:452–467, 2018.

[15] Benedict Lawrence Sy, Zouheir Fawaz, and Habiba Bougherara. Numerical simulation correlating the low velocity impact behaviour of flax/epoxy laminates. *Composites Part A: Applied Science and Manufacturing*, 126:105582, 2019.